K-3-3

Extended Abstracts of the 2013 International Conference on Solid State Devices and Materials, Fukuoka, 2013, pp1006-1007

# GeSn Metal-Semiconductor-Metal Photodetectors with Suppressed Dark Current by Ammonium Sulfide Surface Passivation

Yuan Dong,[1] Wei Wang,[1] Xin Xu,[1] Xiao Gong,[1] Pengfei Guo,[1] Qian Zhou,[1] Lanxiang Wang,[1] Genquan Han,[1] Zhe Xu,[2] Soon-Fatt Yoon,[2] and Gengchiau Liang[1], Yee-Chia Yeo.[1,*]

[1] Department of Electrical and Computer Engineering, National University of Singapore, Singapore 117576.
[2] School of Electrical and Electronic Engineering, Nanyang Technological University, Singapore 639798.
*Phone: +65 6516-2298, Fax: +65 6779-1103, E-mail: yeo@ieee.org

## I. INTRODUCTION

Optical communication based on silicon photonics requires the development of high performance near-infrared (NIR) photodetectors. Germanium-tin (GeSn), as one of the group IV semiconductor alloys, is attracting great interest for applications in NIR photodetectors which can cover all the optical communication bands [1]-[4]. Among all the photodetector structures, metal-semiconductor-metal (MSM) photodetectors exhibit the advantages of the highest response speed and ease of integration [5]. However, MSM photodetectors generally suffer from large dark current, which greatly limits its applications. Therefore, it is important to explore techniques to suppress the dark current of MSM photodetectors.

In this paper, we report, for the first time, the dark current suppression of GeSn MSM photodetectors by a $(NH_4)_2S$ surface passivation. Reduction of dark current as large as 67.2% was achieved with $(NH_4)_2S$ passivation as compared with that of the unpassivated ones, which can be attributed to the -reduction of surface states by $(NH_4)_2S$ surface passivation. Responsivity of 181 mA/W at bias voltage of 3 V was also achieved at the wavelength of 1550 nm.

## II. MATERIAL CHARACTERIZATION

Epitaxial GeSn films were grown on Ge(100) substrate using molecular beam epitaxy (MBE) at 170 °C. Cross-sectional TEM image of a 780 nm-thick GeSn film on Ge(100) substrate is shown in Fig. 1(a). High resolution TEM (HRTEM) image in Fig. 1(b) shows the single-crystalline GeSn film with high crystalline quality. The surface region and interface region of the GeSn film are shown in Fig. 1(c) and (d), respectively. High resolution XRD (HRXRD) (004) and (224) curves in Fig. 2(a) and (c) show that the as-grown GeSn film has a substitutional Sn composition of 2.6%. Fig. 2(b) and (d) are (004) and (224) curves of the GeSn film after 400 °C annealing for 30 minutes in $N_2$ ambient. Negligible change of substitutional Sn composition was observed after annealing, indicating good thermal stability of the as-grown GeSn film. AFM images in Fig. 3(a) and (b) show the RMS surface roughness of the as-grown GeSn film and the one after annealing, respectively. Surface smoothness of the GeSn film was improved by annealing.

## III. DEVICE FABRICATION AND CHARACTERIZATION

### A. Device Fabrication

The process flow for fabricating GeSn MSM photodetectors is shown in Fig. 4(a). Mesa structure was first formed by wet etch after the epitaxial growth of GeSn film. One sample was immersed in a $(NH_4)_2S$ (24%) solution for 1 hour at room temperature for surface passivation. For the control sample, this passivation step was skipped. A 100-nm thick $SiO_2$ layer was then deposited for both of the two samples by sputtering. The inner and outer electrode contact regions were then patterned and opened by wet etch. Right after this, 15 nm-thick Ni was deposited and followed by rapid thermal annealing (RTA) at 350 °C for 30 s to form the NiGeSn metallic contacts. The unreacted Ni was then removed by concentrated sulfuric acid. Finally, Al electrodes were formed by electron-beam evaporator (E-beam) deposition and lift-off.

Top-view SEM image of the GeSn MSM photodetector is depicted in Fig. 4(b). Fig. 4(c) shows the cross-sectional schematic of GeSn MSM photodetector along the dash line A-A' shown in Fig. 4(b). Electrode width ($w$), as defined in Fig. 4(c), was designed to be equal to electrode spacing ($s$) with the values ranging from 6 to 10 μm.

### B. Electrical and Optical Characteristics

*I-V* characteristics of GeSn MSM photodetectors with and without $(NH_4)_2S$ surface passivation are shown in Fig. 5. Electrode spacings of the GeSn MSM photodetectors in Fig. 5(a), (b), and (c) are 10, 8, and 6 μm, respectively. At a bias voltage of 3 V, the dark currents of $(NH_4)_2S$-passivated photodetectors are 67.2%, 50%, and 39% smaller than those of the unpassivated ones, as shown in Fig. 5(a), (b), and (c), respectively. This can be attributed to the reduction of surface states by $(NH_4)_2S$ passivation of the GeSn surface.

The photocurrent of a photodetector is defined as the difference between the total current under illumination and its dark current. Fig. 6 shows the photocurrent of the $(NH_4)_2S$-passivated GeSn MSM photodetectors as a function of bias voltages at different laser powers. Fig. 7 shows the photocurrent of the GeSn MSM photodetectors at different laser powers with and without $(NH_4)_2S$ surface passivation. Difference in photocurrent with and without passivation is very small, which indicates that $(NH_4)_2S$ surface passivation has negligible influence on photocurrent of the GeSn MSM photodetectors.

It is noted that the dark current is still relatively high after surface passivation, which degrades the signal-to-noise ratio (SNR). This is due to Fermi level pinning near the valence band of GeSn, resulting in a small hole Schottkey barrier height (SBH) at the Ni-GeSn/GeSn interface and leading to large hole leakage current. This dark current cannot be suppressed by surface passivation. Therefore, our further investigations will be focused on combination of surface passivation, which reported in this work, with techniques that can increase the hole SBH to improve the SNR.

Fig. 8(a) shows photocurrent of the $(NH_4)_2S$-passivated GeSn MSM photodetectors as a function of bias voltage at different light wavelengths. The wavelengths are 1550, 1580, 1610, and 1630 nm, and the laser power is 1 mW. Fig. 8(b) shows the responsivity-wavelength characteristics of the $(NH_4)_2S$-passivated GeSn MSM photodetectors at a bias voltage of 3 V. A responsivity of 181 mA/W was achieved at the wavelength of 1550 nm.

## IV. CONCLUSION

We demonstrated, for the first time, the dark current suppression of GeSn MSM photodetectors by $(NH_4)_2S$ surface passivation. Maximum suppression of 67.2% was achieved with passivation. The large dark current suppression can be attributed to the reduction of surface states by $(NH_4)_2S$ surface passivation. Responsivity of 181 mA/W was achieved at the wavelength of 1550 nm.

**ACKNOWLEDGEMENT.** The authors acknowledge support from the National Research Foundation under Grant NRF-CRP6-2010-4.

## REFERENCES

**[1]** S. J. Su *et al.*, *Optics Express* 19, 6400, 2011.
**[2]** J. Werner *et al.*, *APL* 98, 061108, 2011.
**[3]** J. Mathews *et al.*, *APL* 95, 133506, 2009.
**[4]** M. Oehme *et al.*, *APL* 101, 141110, 2012.
**[5]** Y. H. Chen *et al.*, *IEEE EDL* 28, 1111, 2007.

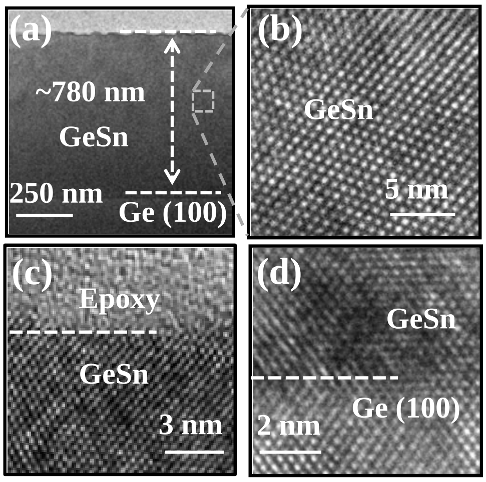


Fig. 1. (a) Cross-sectional TEM image of an epitaxial GeSn film on Ge(100) substrate. HRTEM image of the (b) bulk region, (c) top surface region, and (d) GeSn/Ge interface region of the GeSn film.

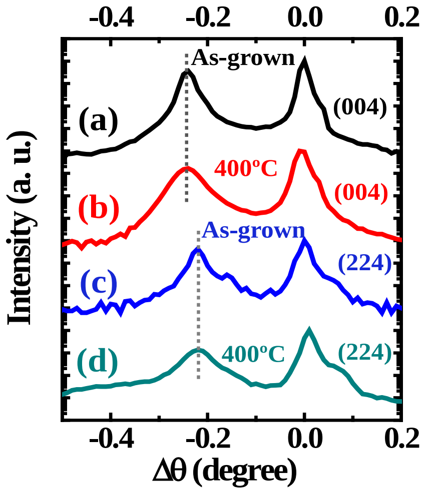


Fig. 2. HRXRD (a) (004) and (c) (224) curves show that the as-grown GeSn film has a substitutional Sn composition of 2.6%. Negligible change of the substitutional Sn composition was observed after 400 ºC RTA for 30 minutes, as shown in HRXRD (b) (004) and (d) (224) curves.

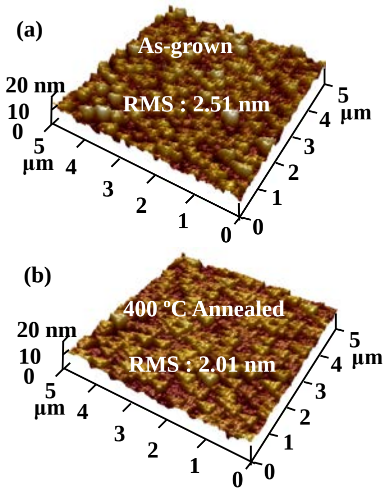


Fig. 3. RMS surface roughness of the (a) as-grown GeSn film and (b) the one after 400 ºC RTA for 30 minutes. RTA improves the surface smoothness of the GeSn film.

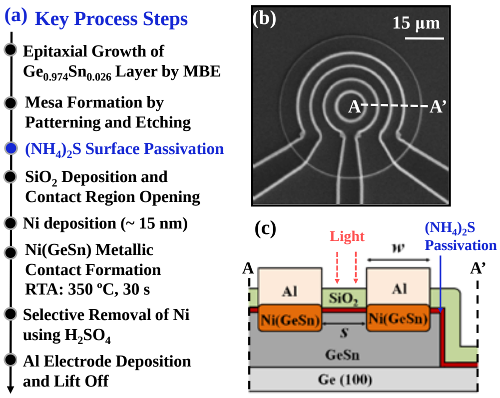


Fig. 4. (a) Key process steps for fabricating the GeSn MSM photodetector with $(NH_4)_2S$ surface passivation. (b) Top-view SEM image of the GeSn MSM photodetector. (c) Cross-sectional schematic of the GeSn MSM photodetector along line A-A' shown in (b). Electrode width ($w$) and spacing ($s$) between electrodes are defined in this figure.

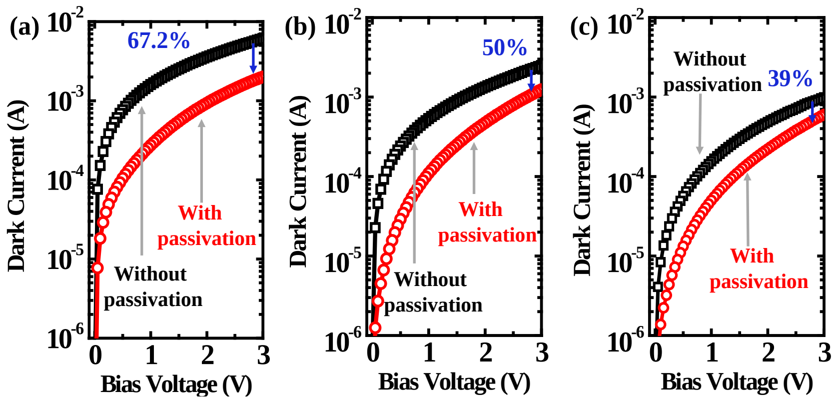


Fig. 5. *I-V* characteristics of the GeSn MSM photodetectors with (a) $w = s = 10$ µm, (b) $w = s = 8$ µm, and (c) $w = s = 6$ µm with and without $(NH_4)_2S$ surface passivation. At a bias voltage of 3 V, the dark currents of $(NH_4)_2S$-passivated photodetectors are 67.2%, 50%, and 39% smaller than those of the unpassivated ones, as shown in (a), (b), and (c), respectively.

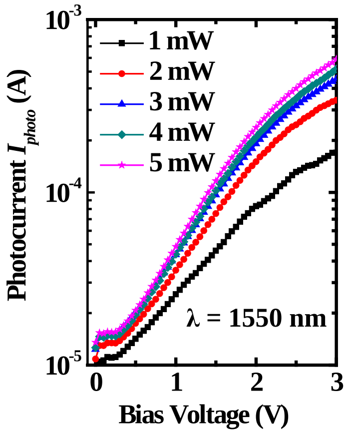


Fig. 6. Photocurrent $I_{photo}$ of the $(NH_4)_2S$-passivated GeSn MSM photodetectors as a function of the bias voltage at different laser power values.

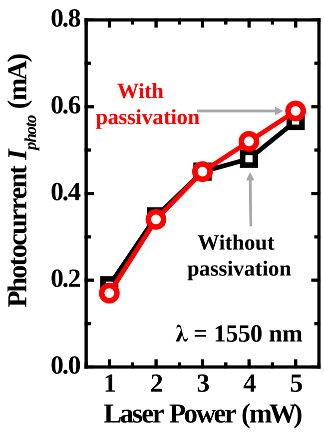


Fig. 7. Photocurrent $I_{photo}$ of the GeSn MSM photodetectors with and without $(NH_4)_2S$ surface passivation at different laser powers. Negligible change of photocurrent was observed.

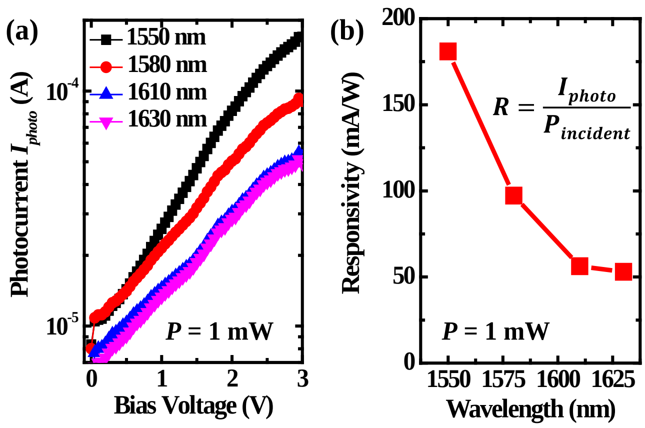


Fig. 8. (a) Photocurrent $I_{photo}$ of the $(NH_4)_2S$-passivated GeSn MSM photodetectors as a function of the bias voltage at different light wavelengths, measured at a laser power of 1 mW. (b) Responsivity-wavelength characteristics of the photodetectors at a bias voltage of 3 V.